2014 International Conference on Unmanned Aircraft Systems (ICUAS)
May 27-30, 2014. Orlando, FL, USA

Control Performance Analysis for Autonomous Close Formation Flight Experiments

Caleb Rice, Yu Gu, Haiyang Chao, Trenton Larrabee, Srikanth Gururajan,
Marcello Napolitano, Tanmay Mandal, Matthew Rhudy

***Abstract*— Close Formation Flight is a key potential approach for reducing greenhouse gas emissions and managing traffic in future high density airspace. This paper discusses the implementation and flight testing of a formation flight controller. Experimental results show that an autonomous close formation flight with approximately 5-wingspan separation is achievable with a pair of low-cost unmanned research aircraft.**

***Keywords*— close formation flight, flight control, UAV, flight testing**

I. Introduction

Autonomous formation fight is an enabling technology for future manned and unmanned aircraft systems. Its potential benefits include energy saving and greenhouse gas reduction [1][2]; improved aircraft coordination within high density airspace [3][4]; as well as mixed operations of Unmanned Aerial Vehicles (UAVs) and manned aircraft [5]. Autonomous formation flight is also the foundation for autonomous aerial refueling [6] and UAV swarm operations [7].

The benefits of Close Formation Flight (CFF) in nature have been well documented. Experimental biology research found that certain birds flying in formation earned a 11.4% - 14.0% energy savings when flying in 'V' shape formation [8][9]. Similar benefits for manned aircraft have also been investigated. NASA researchers at Dryden Flight Research Center demonstrated fuel savings of up to 14% during CFF of two F-18 research aircraft [10] and 10% during CFF of two C-17 aircraft [11]. This research and others [12] also showed that in order to enjoy the aerodynamic benefits, the aircraft has to be precisely controlled at specific locations behind the leader. Therefore, precision computer control for close formation flight is necessary.

Autonomous formation flight control has been explored using a number of different strategies. For space applications formation flight control strategies has been categorized as: 'Multiple-Input Multiple-Output', 'Leader-Follower', 'Cyclic', and 'Behavioral' [12]. Techniques for stability analysis of an autonomous formation have also been developed for measuring how position errors propagate form one vehicle to another in a cascaded system [29][30].

The Leader-Follower approach has been widely accepted for aircraft formation flight due to relative conceptual simplicity where the problem can be represented as tracking problems that can be solved using standard control techniques. Compensation-type controllers [14][15][16][17], optimal control [18][19], adaptive control [20], robust control [21], feedback linearization [22][23], and behavioral [24] approaches have all been developed for formation flight applications.

Experimental demonstrations of autonomous formation flight with fixed-wing aircraft were very limited due to the complexity in multiple aircraft operations. Flight experiments have been conducted by NASA [10][27], DARPA [11], and a few universities [25][26][28].

The research presented in this paper is the first effort in achieving autonomous close formation flight using small fixed-wing unmanned aircraft. The goal of this paper is to evaluate the performance of the designed formation controller from flight test data. Formation control performance is measured by how precisely the pre-specified formation geometry can be maintained under dynamic flight conditions.

This paper will continue in section II with an overview of the formation flight controller design. Section III will discuss about flight testing phases and procedures. Section IV will show the experimental results and then section V will conclude with a discussion of future research directions.

II. Controller Design

Research was focused on a 2-aircraft 'I' shape formation flight control. The aircraft, which are two WVU 'Phastball' unmanned research aircraft, flew in a lead-follower configuration. The leader aircraft was remotely controlled by a ground pilot and the following aircraft were piloted by an onboard formation controller. The controller is designed to maintain a predetermined formation geometry. The formation geometry is defined by a lateral, vertical, and

Caleb Rice is a MS Student at the Department of Mechanical and Aerospace Engineering (MAE), West Virginia University (WVU), PO Box 6106, Morgantown, WV, 26506, crice14@mix.wvu.edu.
Corresponding: Yu Gu is an Assistant Professor at MAE Department, WVU, yu.gu@mail.wvu.edu.
Haiyang Chao is an Assistant Professor at the Aerospace Engineering Department, University of Kansas, chaohaiyang@ku.edu.
Trenton Larrabee is an MS Student at MAE Department, WVU, tlarrab1@mix.wvu.edu.
Srikanth Gururajan is Postdoctoral Fellow at MAE Department, WVU, srikanth.gururajan@mail.wvu.edu.
Marcello Napolitano is a Professor at MAE Department, WVU, marcello.napolitano@mail.wvu.edu.
Tanmay Mandal is a Ph.D. Student at MAE Department, WVU, tmandal@mix.wvu.edu.
Matthew Rhudy is a Visiting Assistant Professor at the Mechanical Engineering Department, Lafayette College, rhudym@lafayette.edu.

forward clearance in the leader aircraft body frame with respect to the position of the leader GPS antenna as shown in Figure 1.

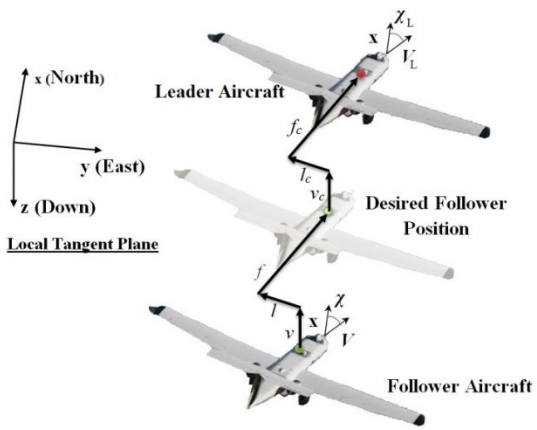

Fig. 1. Formation Flight Geometry

Within Figure 1, the vertical, *v*; lateral, *l*; and forward, *f,* distance errors count off from the predetermined formation clearance, marked by the subscript '$_c$', to the follower's position. These are the performance parameters being analyzed in this experiment. The formation flight controller contains an inner and an outer loop structure. The outer-loop controller minimizes the lateral, forward, and vertical distance errors. It tracks the desired follower position (defined by the formation geometry) behind the leader and provides the desired pitch attitude, throttle position, and roll angle references to the inner-loop controller. The inner-loop control laws then perform the disturbance attenuation and attitude tracking functions.

A. Formation Flight Control Laws

The formation flight controller considered the flight path typically lies in a 2D plane which simplifies flight control into two decoupled horizontal and vertical tracking problems. The position and velocity of the aircraft in formation were expressed with respect to a local tangent plane.

The outer loop control is designed using a nonlinear dynamic inversion (NLDI) approach. Detailed design for the outer loop controller was presented in [26] and the developed nonlinear control laws for the horizontal tracking problem are:

$$\phi_d = \arctan\{\frac{1}{g cos\gamma}\left[\ddot{l}_d \cos(\mathcal{X}-\mathcal{X}_L) + \ddot{f}_d \sin(\mathcal{X}-\mathcal{X}_L)\right] + \frac{V}{g}\Omega_L + \frac{\Omega_L}{g cos\gamma}\left[\dot{l}\sin(\mathcal{X}-\mathcal{X}_L) - \dot{f}\cos(\mathcal{X}-\mathcal{X}_L)\right]\} \quad (1)$$

$$\delta_T = \frac{m}{K_T cos\gamma}\left[\ddot{l}_d \sin(\mathcal{X}-\mathcal{X}_L) + \ddot{f}_d \cos(\mathcal{X}-\mathcal{X}_L)\right] + \frac{1}{K_T}\left[\frac{1}{2}\rho_0 V^2 S(C_{D0} + C_{D\alpha}\alpha_0) + m sin\gamma - T_b\right] - \frac{m}{K_T cos\gamma}\Omega_L\left[\dot{l}\cos(\mathcal{X}-\mathcal{X}_L) - \dot{f}\sin(\mathcal{X}-\mathcal{X}_L)\right] \quad (2)$$

, where, ϕ_d and δ_d are the desired roll angle and thrust commands respectively; m is mass (in kg). g is gravity; α and β are the angle of attack and side slip angle respectively; γ is the flight path angle, and Ω is the aircraft angular turn rate. C_{D0} and $C_{D\alpha}$ are the aerodynamic coefficients for drag. χ is the aircraft azimuth angle. K_T and T_b are constants to be provided by the engine model. Leader parameters are with '$_L$'.

The linearized horizontal formation error dynamics are then controlled with a set of compensator-type linear control laws:

$$\ddot{l}_d = -K_{ls}\dot{l} - K_l l \quad (3)$$

$$\ddot{f}_d = -K_{fs}\dot{f} - K_f f \quad (4)$$

A linear altitude tracker is used to control the vertical geometry by producing a desired pitch angle:

$$\theta_d = -K_v v - K_{vs}\dot{v} \quad (5)$$

, where, θ_d is the desired pitch angle, v is the vertical distance, and K represents gains which are refined through simulation.

The inner loop control laws are obtained by minimizing the cost function, *J*.

$$J = \int_0^\infty (\bar{x}^T Q \bar{x} + \bar{u}^T R \bar{u})\, dt \quad (6)$$

, where u and *x* are the optimized control action and the state of the aircraft respectively. The state involves longitudinal components (angle of attack, α; pitch rate, q; and pitch angle, θ) and latitudinal components (side-slip, β; roll rate, p; roll angle, θ; yaw rate, r; yaw angle, φ). Q and R are positive definite weighting matrices. Then optimized control action is to enable the aircraft to track the desired angles produced by the outer-loop: pitch, θ_d, and roll, ϕ_d, and yaw, φ_d. The control action of the tracker is expressed as

$$u_A = u_R = K_r\phi_d - K_x x \quad (7)$$

and

$$u_E = K_r\theta_d - K_x x \quad (8)$$

for the lateral and longitudinal dimensions respectively. u_A, u_R and u_E are the deflections of the ailerons, rudder, and elevator respectively. K_r is the matrix of feed-forward gains associated with the desired deflection. K_x is the matrix of feedback gains associated with all the states. Through simulation and iterative adjustment, the inner loop gains (equation 7) and then the outer-loop gains (equations 3-5) were refined until desirable performance was achieved. The refined gains are shown in Table 1.

TABLE I. INNER LOOP GAINS

	Longitudinal	Lateral	
Inner-Loop Controller	K_x = [0.0991, 0.1308, 0.6325]	K_x =[-0.1665, 0.045, 0.0413, 0.5385; -0.0827, 0.0076, 0.1708, 0.1171]	
	K_r=[-0.6325]	K_r=[-0.5413; -0.0147]	
Out-Loop Controller	Forward	Lateral	Vertical
	K_{fs}=1.2 K_f=0.45	K_{ls}=1.7 K_l=0.6	K_{vs}=0.8 K_v=1.3

B. Test bed Aircraft and Avionics

The basic parameters for the West Virginia University (WVU) Phastball aircraft are shown in Table 2. The

Phastball aircraft has a 'T' tail configuration where the horizontal surface is positioned high above the downwash produced by the wings. The propulsion system is comprised of two brushless electric ducted fans that are positioned on the fuselage behind the wings.

TABLE II. BASIC PHASTBALL AIRCRAFT PARAMETERS

Wingspan	2.4 m
Length	2.2 m
Height	0.55 m
TO Weight	10.5 kg
Cruise Speed	32 m/s
Max Flight Duration	480 seconds

The follower's onboard 5^{th} generation avionics [32], Gen-V system, features a custom flight computer, nose sensor suite, IMU, control signal distribution board, R/C sub-system, communication sub-system, power sub-system, and real-time software. An onboard GO-PRO® camera records point of view video. Figure 2 displays the follower aircraft avionics and components.

The Gen-V flight computer performs data acquisition, signal conditioning, and signal distribution as well as flight control and failure accommodation functions [32]. It is capable of integrating and distributing control command from five different sources: ground R/C safety pilot, ground research pilot, aircraft on-board flight control system, on-board failure emulation system, and an On-Board Excitation System (OBES). Safety of the research aircraft is reinforced by several design features, such as hardware redundancies on critical components.

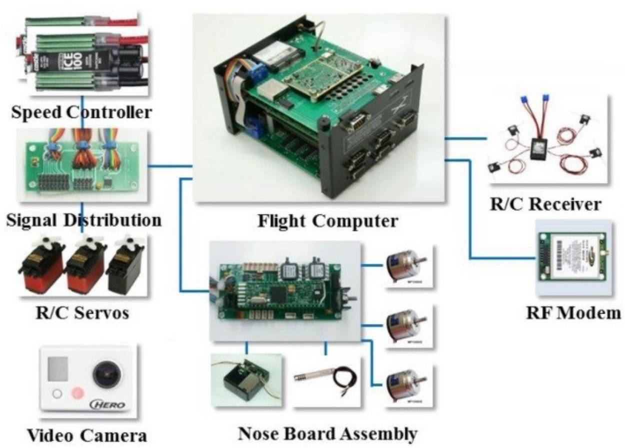

Fig. 2. The Gen-V Avionics System [32].

The leader aircraft has a different type of avionics on-board, which is mostly used for data acquisition and communication. During the flight, the leader aircraft sends out its 3-axis position and velocity information to the follower aircraft through a pair of 900Mhz Freewave RF modems.

III. FLIGHT TESTING

Initial flight tests with a single aircraft were performed for validating the hardware, communication, and inner loop controller performance. The validation of the fully developed formation flight controller was conducted first with a pre-recorded leader aircraft's GPS trajectory around the airfield. Later, flight tests were conducted using a real leader aircraft and one follower aircraft.

Three 2-aircraft formation flights and 10 2-aircraft close formation flights (with a separation at around 5 wingspans) were performed with the Phastball aircraft. Figure 3 pictures the leader and follower in flight. The leader aircraft maintained an oval flight path over the airfield. Once the aircraft rendezvoused in the air, the formation flight control laws were activated and the follower maintained formation as shown in Figure 4.

Fig. 3. Aircraft Demonstrating Close Formation Flight

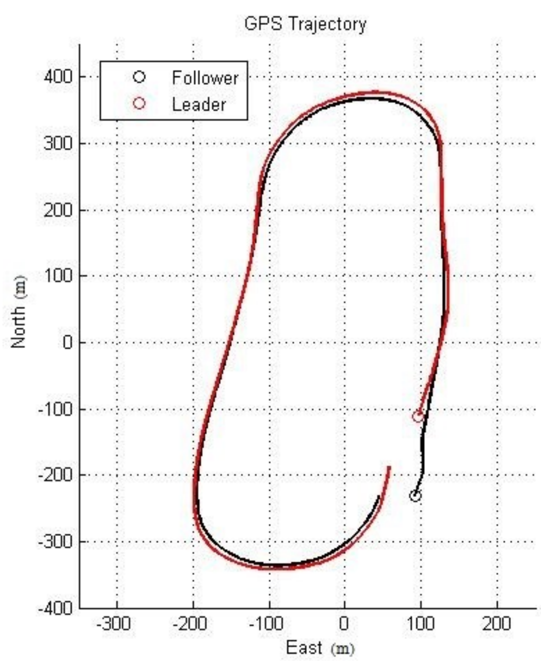

Fig. 4. Oval Flight Path of a Single Lap in Formation

IV. RESULTS

A. Phastball Formation Flight Data Analysis

Only seven flights of 13 were applicable for steady state error analysis. Flights 1, 2, and 3 are not considered close formation flights, for their forward clearance was 50m, 40m, and 30m respectively. Flights 4, 6, and 9 were conducted with variable formation geometry to evaluate transient behaviors. Figure 5 illustrates what the errors look like over the course of a single lap.

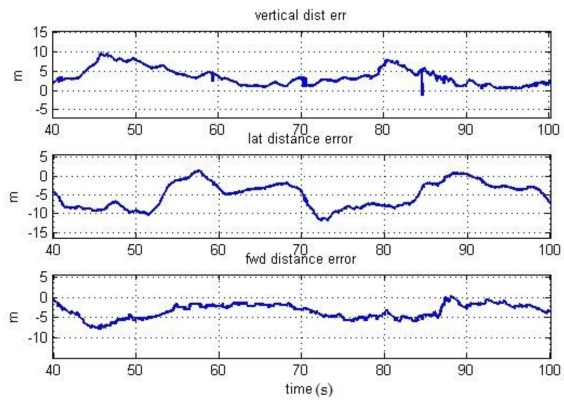

Fig. 5. Formation Flight Errors of a Single Lap

The transient response, illustrated in Figure 6 for the forward distance error, is characterized for all dimensions in Table 3. In Figure 6, the desired forward clearance, red line, decreased from 10-wingspan (24m) to 5-wingspan (12m) in approximately 20 seconds.

The steady state error analyses are shown for the straight legs and turning in Tables 4 and 5 respectively. Straight leg performance is significantly better, especially in the vertical dimension. The average forward error is -0.82 meters meaning the controller is maintaining a closer than desired formation geometry. The average vertical error distance of 1.34 meters means the follower is tracking lower than desired.

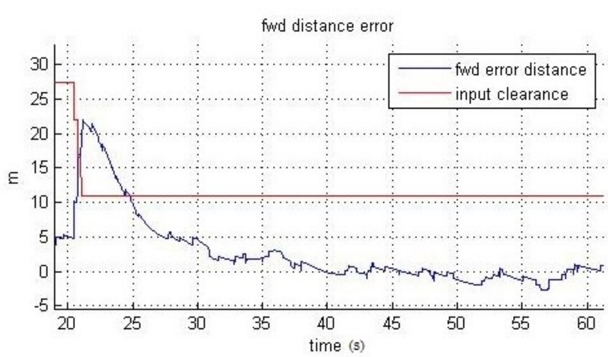

Fig. 6. Transient Response in Forward Distance Error

Along the straight legs, the average magnitude of mean distance error from the close formation flights of Table 4 is 1.33 meters with a standard deviation of 0.88 meters. It should be noted that the steady state error calculation does not consider GPS errors, which is rated for 1.5m RMS and could reach much higher values occasionally during the flight.

In the turns, the average magnitude of mean distance error from Table 5 is 7.54 meters with a standard deviation of 1.68 meters. Table 6 displays the proximity between the leader and follower to give a better depiction of the formation flight geometry.

TABLE III. TRANSIENT BEHAVIOR FROM THE INITIATION OF FORMATION FLIGHT

Transient Behavior		Init. Err. Dist-ance (m)	T react (s)	T peak (s)	T rise (s)	T settlin g (s)	OS%
Flight 5	Vrt	10.00	6.00	7.96	5.06	7.44	2.48%
	Lat	-6.54	5.38	n/a	3.41	4.05	n/a
	Fwd	5.43	0.73	3.36	0.93	1.10	40.19%
Flight 7	Vrt	0.70	0.30	n/a	1.44	1.67	n/a
	Lat	--	--	--	--	--	--
	Fwd	12.22	6.17	n/a	7.76	9.16	n/a
Flight 8	Vrt	10.05	2.10	n/a	3.22	3.80	n/a
	Lat	5.15	7.02	11.12	18.20	18.43	236.23%
	Fwd	7.26	21.76	n/a	27.37	32.30	n/a
Flight 10	Vrt	0.53	1.38	1.72	0.97	2.95	228.30%
	Lat	8.88	4.10	n/a	5.67	6.69	n/a
	Fwd	20.54	32.44	n/a	29.8	35.21	n/a
Flight 11	Vrt	3.99	3.50	5.28	5.10	6.79	29.02%
	Lat	14.53	3.60	n/a	4.65	4.92	n/a
	Fwd	130.0	22.50	18.94	22.5	26.58	14.62%
Flight 12	Vrt	--	--	--	--	--	--
	Lat	77.58	4.07	6.78	6.48	13.30	18.16%
	Fwd	16.72	13.54	n/a	12.7	15.01	n/a
Flight 13	Vrt	10.10	2.32	4.20	4.03	11.40	37.54%
	Lat	23.18	8.50	11.10	9.16	10.81	0.00%
	Fwd	16.27	9.24	n/a	11.9	12.30	n/a

TABLE IV. PERFORMANCE OF THE PHASTBALL 2-AIRCRAFT FORMATION FLIGHT DURING THE STRAIGHT LEGS

FF Straight legs (m)		Clear-ance	Max Err. Dist-ance	Mean Abs. Err. Distance	Mean Err. Dist-ance	Std. Dev.
Flight 5	Forward	12.0	1.087	0.394	0.345	0.331
	Lateral	0.0	1.890	1.303	-1.303	0.286
	Vertical	0.0	3.017	2.295	2.295	0.356
Flight 7	Forward	12.0	1.899	0.649	-0.499	0.596
	Lateral	1.2	0.551	0.184	-0.021	0.238
	Vertical	2.4	2.229	1.640	1.640	0.212
Flight 8	Forward	12.0	1.529	0.536	-0.143	0.596
	Lateral	1.2	1.083	0.606	-0.606	0.225
	Vertical	2.4	2.027	1.302	1.302	0.327
Flight 10	Forward	12.0	3.563	1.763	-1.521	1.239
	Lateral	1.2	0.386	0.129	-0.023	0.157
	Vertical	2.4	2.350	1.696	1.696	0.368
Flight 11	Forward	12.0	2.463	1.168	-0.904	1.020
	Lateral	2.4	1.601	0.630	-0.630	0.469
	Vertical	2.4	1.145	0.434	-0.340	0.397
Flight 12	Forward	12.0	2.637	1.510	-1.510	0.787
	Lateral	2.4	1.041	0.619	-0.619	0.280
	Vertical	2.4	1.815	1.293	1.293	0.317
Flight 13	Forward	12.0	2.686	1.542	-1.526	0.749
	Lateral	2.4	0.795	0.214	-0.148	0.286
	Vertical	2.4	1.885	1.545	1.545	0.137

TABLE V. PERFORMANCE OF THE PHASTBALL 2-AIRCRAFT FORMATION FLIGHT DURING TURNS

FF Turns (m)		Clear -ance	Max Err. Dist-ance	Mean Abs. Err. Distance	Mean Err. Distance	Std. Dev.
Flight 5	Forward	12.0	1.986	0.762	0.729	0.445
	Lateral	0.0	3.438	2.394	2.394	0.524
	Vertical	0.0	9.485	3.960	3.960	1.052
Flight 7	Forward	12.0	2.951	1.863	1.863	0.445
	Lateral	1.2	4.177	3.180	3.180	0.469
	Vertical	2.4	6.812	4.265	4.265	1.380
Flight 8	Forward	12.0	6.059	3.431	3.431	1.307
	Lateral	1.2	4.402	3.836	3.836	0.221
	Vertical	2.4	8.423	5.994	5.994	1.015
Flight 10	Forward	12.0	3.338	0.949	0.818	0.885
	Lateral	1.2	4.512	3.561	3.561	0.479
	Vertical	2.4	11.39	8.718	8.718	1.585
Flight 11	Forward	12.0	3.401	0.972	0.955	0.904
	Lateral	2.4	6.449	4.878	4.878	0.660
	Vertical	2.4	5.019	3.811	3.811	0.960
Flight 12	Forward	12.0	2.030	0.777	0.567	0.753
	Lateral	2.4	4.778	4.264	4.264	0.412
	Vertical	2.4	13.09	10.773	10.773	2.187
Flight 13	Forward	12.0	2.492	1.082	0.747	1.152
	Lateral	2.4	5.584	4.719	4.719	0.557
	Vertical	2.40	7.298	5.454	5.454	1.032

TABLE VI. PROXIMITY BETWEEN LEADER AND FOLLOWER DURING FORMATION FLIGHT

Aircraft Proximity During FF							
		Straight legs			Turns		
	Clear -ance (m)	Max (m)	Min (m)	Mean (m)	Max (m)	Min (m)	Mean (m)
Flight 5	12.2	16.41	14.43	15.42	22.52	14.48	18.50
Flight 7	12.3	15.28	13.56	14.42	20.82	15.54	18.17
Flight 8	12.3	15.06	12.88	13.97	23.57	13.42	18.49
Flight 10	12.3	16.58	13.33	14.96	24.10	18.63	21.81
Flight 11	12.5	15.62	12.48	14.05	21.32	16.64	18.98
Flight 12	12.5	15.84	13.26	14.55	26.56	19.70	23.13
Flight 13	12.5	15.85	13.74	14.79	21.99	17.65	19.82

V. CONCLUSION

Close formation flight was proved to be achievable with a pair of low-cost test bed aircraft and the formation flight controller behaved desirably in these experiments. Formation flight was previously demonstrated with the WVU YF-22 sub-scale aircraft [26] where the magnitude of the mean distance error was found to be 13.52m for a circular flight pattern. The Phastball performed substantially better than the YF-22 during the formation flight. Known factors that brought about this improvement are: electric motors are more responsive over the YF-22's gas turbines and also improved avionics, state estimation, and controller tuning for the Phastball aircraft.

As expected, the designed controller performs better during straight flight than turning. Having the horizontal and vertical dimensions decoupled limits the tracking capabilities when the leader implements a turn, climb, or deceleration. The design could be improved by deriving the 3D formation control laws without decoupling the vertical and horizontal components.

The benefits of formation flight can only be enjoyed if aircraft are precisely controlled. This experiment will contribute to the future of close formation flight research for energy saving and improved air traffic management.

ACKNOWLEDGMENTS

This research was partially supported by NASA grant NNX13AB74A and the West Virginia Space Grant Consortium.

REFERENCES

[1] Blake, W.; Bieniawski, S. & Flanzer, T., "Surfing Aircraft Vortices for Energy," *The Journal of Defense Modeling and Simulation: Applications, Methodology, Technology*. Sep. 11, 2013.

[2] Agarwal, Ramesh K. "Review of Technologies to Achieve Sustainable (Green) Aviation," *Recent Advances in Aircraft Technology*. (2012): 427-464.

[3] Xue, M. & Hornby, G., "An Analysis of the Potential Savings from Using Formation Flight in the NAS," *AIAA Guidance, Navigation, and Control Conf*. Minneapolis, MN, Aug. 2012. doi:10.2514/6.2012-4524.

[4] Jenkinson, L.; Caves , R. & Rhodes, D. "Automatic Formation Flight: A preliminary Investigation into the Civil Operations," IEEE Control Systems, vol.20, no.6, pp.34,44, Dec 2000.

[5] Yang, A.; Naeem, W.; Irwin, G.W. & Kang Li, "A decentralised control strategy for formation flight of unmanned aerial vehicles," Control (CONTROL), *2012 UKACC International Conference*. Cardiff, United Kingdom, 3-5 Sept. 2012. pp.345,350.

[6] Ewers, D., "AARD - Autonomous Airborne Refueling Demonstration," Presented at the East Coast SETP Symposium. Arlington, VA, April. 2007.

[7] Duan, H.; Luo, Q.; Shi, Y. & Ma, G. "Hybrid Particle Swarm Optimization and Genetic Algorithm for Multi-UAV Formation Reconfiguration," *IEEE Computational Intelligence Magazine*, vol.8, no.3, pp.16,27, Aug. 2013.

[8] Weimerskirch, H.; Martin, J.; Clerquin, Y.; Alexandere, P. & Jiraskova, S. "Energy Savings in Flight Formation." *Nature*. Vol. 413, pp. 697-698.

[9] Cutts, C., & J. Speakman. "Energy Savings in Formation Flight of Pink-Footed Geese." *Journal of Experimental Biology* 189.1, 1994, pp. 251-261.

[10] Ray, R.; Cobleigh, B.;, Vachon, M. & StJohn, C. "Flight test techniques used to evaluate performance benefits during formation flight." *Flight Mechanics Conf.*, Monterey, CA. 2002.

[11] Pahle, J., Berger, D., Venti, M. W., Faber, J. J., Duggan, C., & Cardinal, K., "A Preliminary Flight Investigation of Formation Flight for Drag Reduction on the C-17 Aircraft," Presented at the Aerospace Control and Guidance Systems Committee; Salt Lake City, UT; 7 Mar. 2012.

[12] Brodecki, M.; Subbarao, K. & Chu, Q. "Formation Flight Control System for In-Flight Sweet Spot Estimation." *51st AIAA Aerospace Sciences Meeting*. Grapevine, TX, Jan 2013.

[13] Scharf, D.; Hadeagh, F. & Ploen, S. "A survey of spacecraft formation flying guidance and control (part II): control," *American Control Conf.*. Boston, MA, June 2004, pp. 2976-2985.

[14] Dargan, J.; Patcher, M. & D'Azzo, J.J., "Automatic Formation Flight Control," *Proc. AIAA Guidance, Navigation, and Control Conf.*, Hilton Head, SC, Aug. 1992, pp. 838-857.

[15] Buzogany, L.E.; Patcher, M. & D'Azzo, J.J., "Automatic Control of Aircraft in Formation Flight," *Proc. AIAA Guidance, Navigation, and Control Conf.*. Monterey, CA, Aug. 1993, pp. 1349-1370.

[16] Veth, M.; Patcher, M. & D'Azzo, J.J., "Energy Preserving Formation Flight Control," *AIAA Aerospace Sciences Meeting and Exhibit*, Reno, NV, Jan. 9-12, 1995.

[17] Reyna, V.P.; Patcher, M. & D'Azzo, J.J., "Formation Flight. Control Automation," *Proc. AIAA Guidance, Navigation, and Control Conf.*, pp. 1379-1404.

[18] McMammish, S.; Patcher, M. & D'Azzo, J.J., "Optimal Formation Flight Control," *AIAA Guidance, Navigation, and Control Conf.*. San Diego, CA, Jul. 1996.

[19] Dogan, A.; Sato, S. & Blake W., "Flight Control and Simulation for Aerial Refueling," Proc. AIAA Guidance, Navigation, and Control Conference, San Francisco, Aug 15-18, 2005.

[20] Boskovic, J.D. & Mehra, R.K., "An Adaptive Reconfigurable Formation Flight Control Design," *Proc. American Control Conference*. June 2003 Vol 1, pp. 284-289.

[21] Li, Y.; Li, B.; Sun, Z. & Song, Y.D, "Robust Autopilot for Close Formation Flight of Multi-UAVs, System Theory," *Proc. from the Thirty-Eigth Southeastern Symposium*, March 2006, pp. 258-262.

[22] Singh, S.N.; Chandler, P.; Schumacher, C.; Banda, S. & Pachter M., "Adaptive Feedback Linearizing Nonlinear Close Formation Control of UAVs," *Proc. American Control Conference*, 2000. Vol. 2, pp. 854-858.

[23] Venkataramanan, S. & Dogan, A, "Nonlinear Control for Reconfiguration of UAV Formation," *Proc. AIAA Guidence, Navigation, and Control Conference*, Austin, TX, Aug. 2003.

[24] Fabrizio, G.; Pollini, L. & Innocenti, M., "Formation flight control - A behavioral approach," *AIAA Guidance, Navigation, and Control Conference and Exhibit.* Montreal, CA, Aug. 2001.

[25] Johnson, E.N.; Calise, A.J.; Sattigeri, R. & Watanabe, Y., "Approaches to Vision-Based Formation Control," *Proc. IEEE Conference on Decision and Control,* December 2004.

[26] Gu, Y., Campa, G., Seanor, B., Gururajan, S., & Napolitano, M. R., "Autonomous formation flight–design and experiments." Aerial Vehicles, 2009, pp. 233-256.

[27] Hanson, C.E.; Ryan, J.; Allen, M.J. & Jacobson, S.R., "An Overview of Flight Test results for a Formation Flight Autopilot," *AIAA Paper* 2002-4755, Aug. 2002.

[28] How, J.P.; King, E. & Kuwata, Y., "Flight Demonstration of Cooperative Control for UAV teams," *Proc. AIAA 3rd Unmanned unlimited technical Conference, Workshop and Exhibit,* Sept. 2004. AIAA-2004-6490.

[29] Allen, M.J.; Ryan J.; Hanson, C.E. & Parle, J.F., "String Stability of a Linear Formation Flight Control System," AIAA Paper 2002-4756, National Aeronautics and Space Administration, Dryden Flight Research Center, Aug. 2002.

[30] Giulietti, F.; Pollini, L.; Innocenti, M. "Autonomous Formation Flight." *IEEE Control Systems Magazine,* Dec. 2000, 34-44.

[31] Tancredi, D., Gu, Y., and Chao, H. "Fault tolerant formation flight control using different adaptation techniques." Unmanned Aircraft Systems (ICUAS), 2013 International Conference on. IEEE, 2013.

[32] Gu, Y., Gross, J., Barchesky, F., Chao, H.Y., and Napolitano, M.R., "Avionic Design for a Sub-Scale Fault Tolerant Flight Control Test-Bed," Chapter 21, Recent Advances in Aircraft Technology, ISBN: 978-953-51-0150-5, InTech, pp. 499-522, 2012.